Journal of Materials Science: Materials in Engineering

ORIGINAL PAPER

Open Access

Experimental study of characterization and optimization of shape memory alloy sheet for enhanced mechanical actuation performance for microelectromechanical systems (MEMS)

Suraj[1*] and Arun Kumar[1]

Abstract

In this paper, a shape memory alloy (SMA), NiTiNOL, zigzag sheet is used and experimental method is developed using programmable power supply, laser displacement sensor, and K-type thermocouple to investigate actuation and thermo-mechanical behavior of trained SMA zigzag sheet under three different weights, 2.5 N, 3.5 N, and 4.5 N, along with three distinct voltage levels 2.0 V, 3.0 V, and 4.0 V and hysteresis curves are comprehensively examined to get optimum value of load and voltage to achieve better life cycle and actuation as per the requirement of the design. The displacement and temperature data of the zigzag sheet is recorded for every 200 ms for the entire operating life, utilizing heating and cooling processes, of the zigzag sheet and the value of constant displacement for each cycle is optimized which can be used for the development of microelectromechanical systems (MEMS).

Keywords Smart material, Shape memory alloy sheet, NiTiNOL, Actuation, Thermo-mechanical characteristics, Design innovation

Introduction

Over the past few decades, there have been extensive discussions regarding the rapid responsiveness of shape memory alloys (SMAs) (Lagoudas 2008; Sun et al. 2012; Namazu et al. 2006; Basit et al. 2013; Takashima et al. 2014; Pimpin et al. 2004; Pelrine et al. 1998; Chen and Liu 2013; Jayaram et al. 2018; Grunwald and Olabi 2008; Hong 2013). NiTi has gained considerable attention among researchers due to its unique properties, such as the shape memory effect, super-elasticity, high damping capacity, substantial kinetic output, noise-free operation, and the highest actuation force compared to various other actuators (Yuan et al. 2017; Mohd Jani et al. 2016; Patil and Song 2017; Sun et al. 2016; Moiseev 2005; Teh 2008; Bale et al. 2023; Cao et al. 2023; Shape memory alloys - new advances [working title]. 2023; Mehta et al. 2024; Gangwar et al. 2023; Mobarak et al. 2023; Nithyanandh et al. 2023; Jain et al. 2022; Nath and Kumar 2021; Kim et al. 2023; Chaudhary et al. 2024; Dzogbewu and Johan 2024). In this chapter, a unique experimental setup has been developed to estimate the life cycle of SMAs through electrical actuation. The hysteresis response of NiTi is intricately linked to both the applied load and temperature. The estimation of the life cycle of SMA involves the utilization of heating and cooling processes, with Joule heating serving a crucial role in SMA actuation. The activation of SMA material occurs through Joule heating and is suggested for diverse applications, as elaborated upon

*Correspondence:
Suraj
suraj.ph21.me@nitp.ac.in
[1] Department of Mechanical Engineering, National Institute of Technology Patna, Patna, Bihar, India

below. The experimental parameters that have undergone variation include voltage, load, and displacement.

Experimental setup and experimentation

1. Experimental setup: A test setup was created to explore the thermo-mechanical responses induced by Joule heating in an SMA actuator. In the course of the life cycle analysis, the SMA actuator underwent repeated cycles of heating and cooling until failure was evident. The investigation was complemented by employing various characterization techniques to validate the observations. The thermo-mechanical fatigue of the sheet was evident, and as the cycles increased, it became apparent that the fabricated trained SMA sheet experienced inelastic deformation, leading to their inability to return to their original shape. SMA fatigue behavior is typically assessed through three distinct approaches (Chang and Read 1951). Firstly, fatigue-induced fractures can occur due to stress or strain cycling at a consistent temperature. Secondly, changes in physical, mechanical, and memory properties may manifest through pure thermal cycling across the transformation region. Thirdly, a combination of thermal cycling through the transformation region and constant stress or strain loading can lead to variations in physical, mechanical, and memory properties. The third type of fatigue behavior, prevalent in many mechanical applications, is the focus of consideration in this context. To address this, an experimental setup was devised and implemented to collect data from the initial stage to the point of failure. Figure 1 illustrates the schematic overview and actual photographs of the experimental arrangement.
2. Experimentation: The setup employed a laser displacement sensor (LDS), a K-type thermocouple, programmable power supply (PPS), an external weight applied using a pulley system, and the fabricated NiTi SMA zigzag sheet. The NiTi SMA zigzag sheet was acquired to explore the life characteristics of the zigzag sheet, and its specifications for the current case study are detailed in Table 1.

The zigzag sheet, which is one-way trained, contracts upon actuation, specifically the application of voltage. To maintain the extended position, an external load is applied to the spring. The programmable power supply (PPS) not only delivers the specific energy required for the phase transformation of the zigzag sheet but also plays a crucial role in controlling the heating and cooling cycles of the zigzag sheet. At the experiment's outset, a weight was applied to the sheet to maintain its extended position. Subsequently, a voltage (V_c) was applied to the sheet through the programmable power supply (PPS). The sheet, upon receiving the voltage, recovered its original length against gravity by lifting the weights. Following the recovery phase, the voltage was cut off, allowing the sheet to cool at room temperature. During the cooling process, external weight was applied to the sheet, exerting force for the sheet to revert to its deformed shape. Iterative steps were undertaken to calculate the time required for the heating and cooling cycles of the SMA zigzag sheet. The heating and cooling phases of the zigzag sheet collectively constitute the actuation. The cumulative actuation over one cycle is essential for measuring the life cycle of the zigzag sheet. The reduction in elongation observed over the number of cycles serves as an indicator of failure. The elongation of the zigzag sheet was quantified using the laser displacement sensor (LDS), while a K-type thermocouple was affixed to measure the temperature during both actuation and the release of the zigzag sheet. For actuation analysis, conducting experiments on a sheet with consistent mechanical properties involved the application of

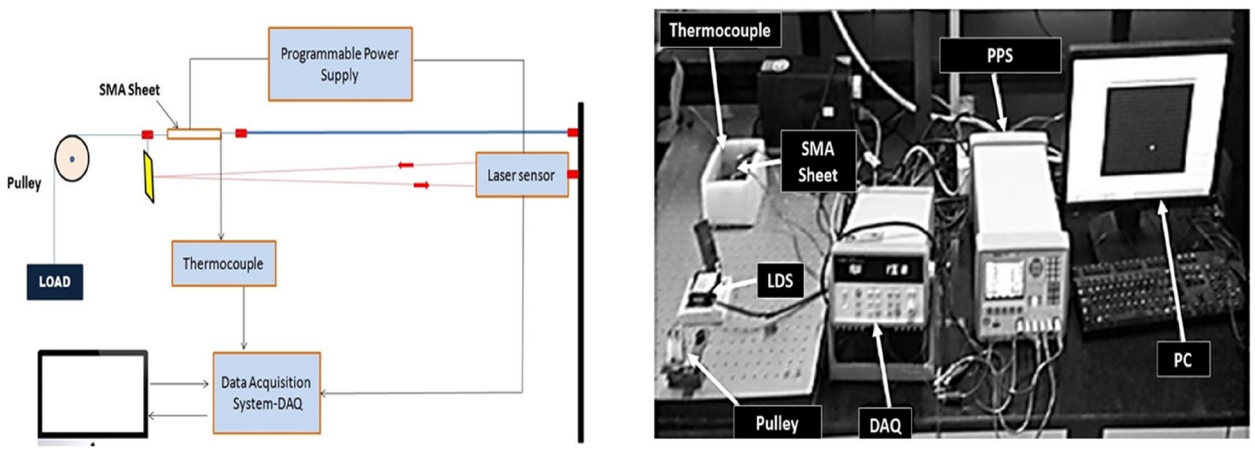

Fig. 1 Line diagram and experimental setup for SMA actuation for Joule heating

Table 1 One-way trained SMA sheet specifications

Complete length of sheet length (l)	Sheet breath (b)	Sheet thickness (t)	Number of zigzag (n)
31.5 mm	2.5 mm	0.5 mm	4.5

various voltage waveforms. Throughout each experiment, data on sheet displacement and temperature was meticulously recorded at intervals of 200 ms, spanning the entire operational lifespan of the sheet. The investigation into the thermo-mechanical behavior was conducted under three different weights, namely 2.5 N, 3.5 N, and 4.5 N, along with three distinct voltage levels—2.0 V, 3.0 V, and 4.0 V.

The sample underwent scanning electron microscopy to analyze alterations in its life cycle in response to varying weights and voltages (Chouhan et al. 2016).

Result and discussion

For thermo-mechanical behavior (displacement vs. time curve) and temperature vs. time curve and for actuation behavior, the hysteresis curve at 3 different weights at 2.5 N, 3.5 N, and 4.5 N at 2 V, 3 V, and 4 V is investigated providing a comprehensive depiction of the cyclic behavior under varied loading conditions.

Thermo-mechanical behavior (displacement vs. time curve) and temperature vs. time curve at 3 different

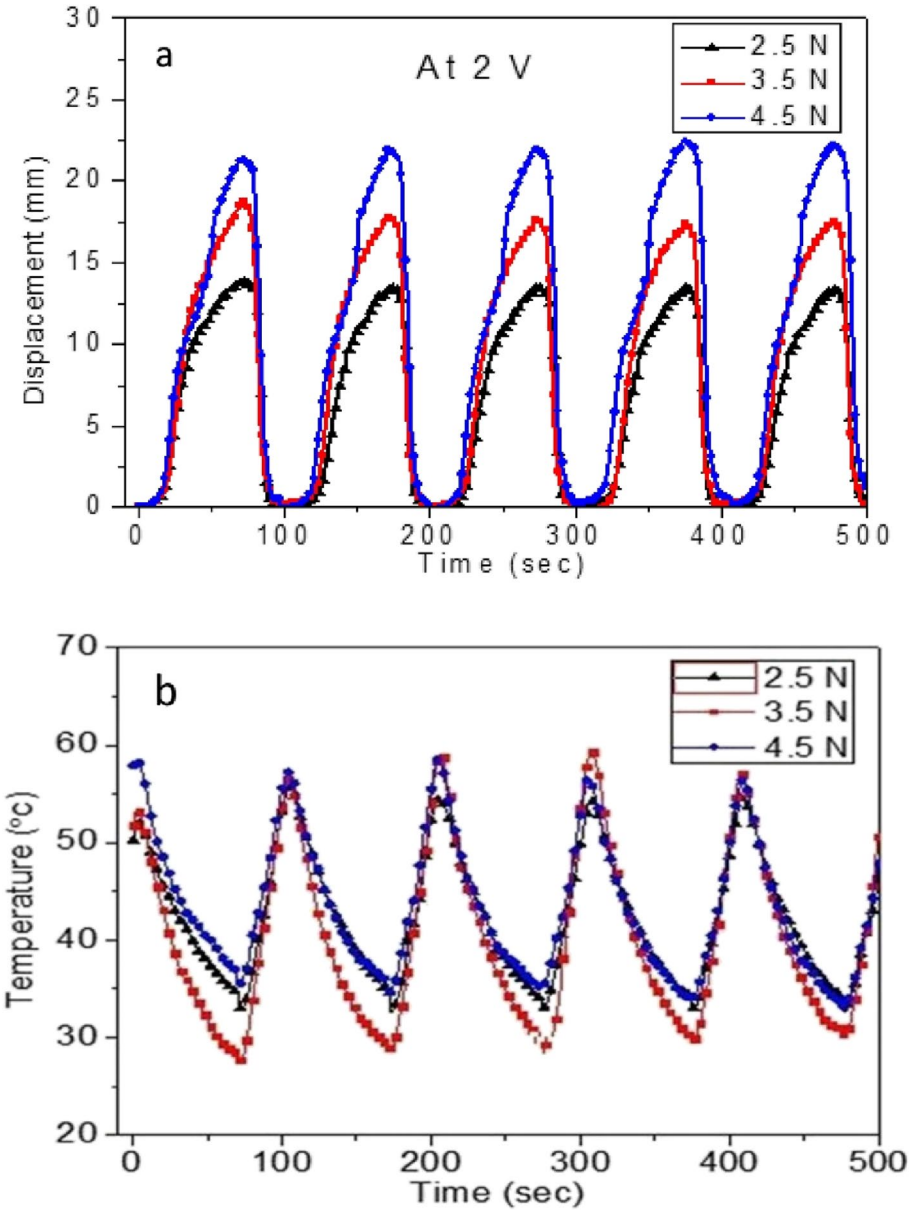

Fig. 2 Displacement vs. time at 2.0 V for different weight **a** for 2.5 N, 3.5 N, and 4.5 N, **b** temperature vs. time plot for 2.5 N, 3.5 N, and 4.5 N

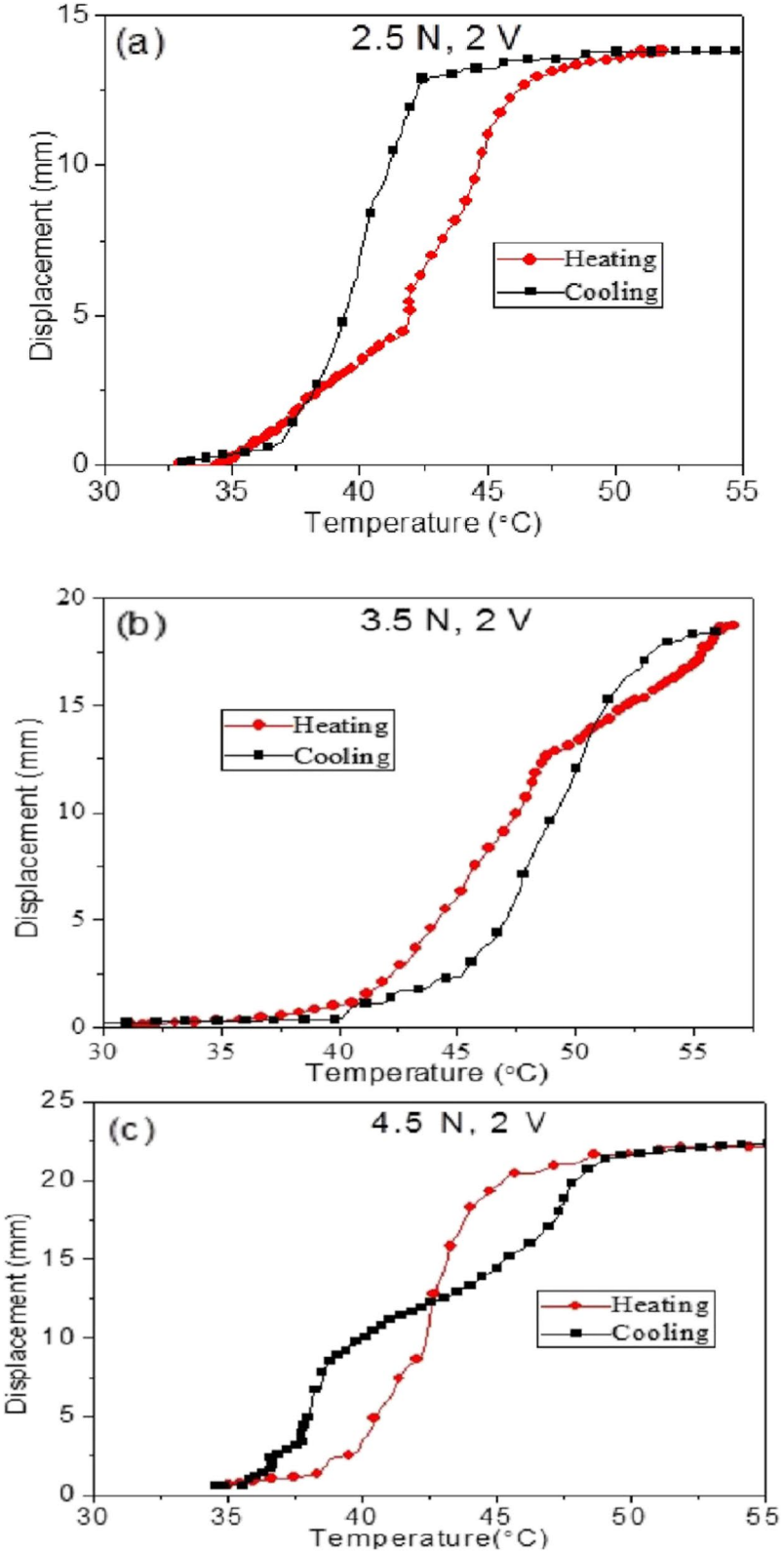

Fig. 3 Hysteresis curve for actuation of SMA at 2.0 V and **a** 2.5 N, **b** 3.5 N, and **c** 4.5 N

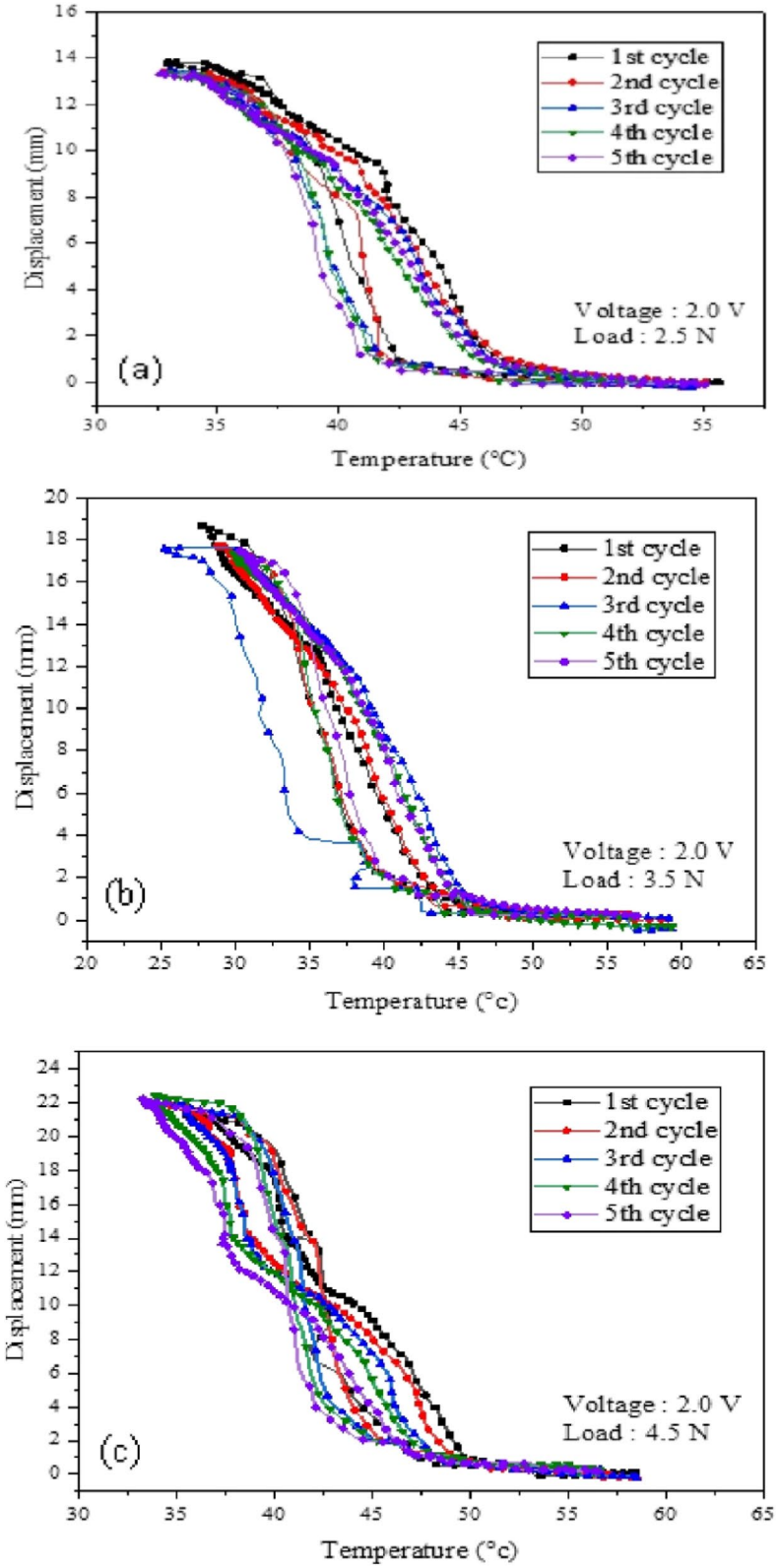

Fig. 4 Hysteresis curves for five cycles are depicted at a voltage of 2.0 V under varying loads: **a** 2.5 N, **b** 3.5 N, and **c** 4.5 N

weights at 2.5 N, 3.5 N, and 4.5 N at 2 V is shown in Fig. 2.

In Fig. 3, actuation behavior, the hysteresis curve at 2 V is illustrated for different applied weights, specifically 2.5 N, 3.5 N, and 4.5 N, providing a comprehensive depiction of the cyclic behavior under varied loading conditions.

Figure 4 displays hysteresis curves for five cycles at a voltage of 2.0 V under different loads (2.5 N, 3.5 N, and 4.5 N). It is worth noting that, due to the utilization of a zigzag sheet in the test bench, the possibility of the sheet behaving in a reversed manner should be considered.

In Fig. 5, the thermo-mechanical response of SMA, represented by the displacement versus time graph, is depicted under varying loads of 2.5 N, 3.5 N, and 4.5 N, with an applied voltage of 3.0 V, particularly when the zigzag sheet is subjected to loading. Additionally, Fig. 5 also includes the temperature versus time graph for the corresponding cycle. Furthermore, the actuation behavior for a single cycle is illustrated in Fig. 6. In Fig. 7, hysteresis curves for five cycles are presented, specifically at a voltage of 3.0 V, under identical loading conditions.

When the sheet was activated with a voltage of 4.0 V under consistent loading conditions, the displacement exhibited a range between 10 and 15 mm. This process was iteratively repeated five times, and the corresponding thermo-mechanical behavior and hysteresis curve are illustrated in Figs. 8 and 9.

Corresponding temperatures were measured using a K-type thermocouple within the range of 30 to 60 °C. At the 2.5 N weight, the displacement recorded was 15.10 mm with a temperature of 54.49 °C, which increased to 18.32 mm at 3.5 N with a temperature of 58.69 °C. The maximum displacement of 21.25 mm was achieved at 4.5 N with a corresponding temperature of 58.93 °C. Time taken for heating and cooling and to attain a constant displacement for each cycle, the optimal values were determined and tabulated as shown in Table 2.

Observing all hysteresis curves, a distinct point of intersection is evident in each. Specifically, in Fig. 2, this intersection occurs at 12.74 mm, attributed to a phase transition. Although imperceptible during the heating phase, as the cooling commenced, the transition from austenite to martensite became apparent, leading to the crossing of curves and the resulting intersection. Plots for displacement and time, temperature and time, as well as hysteresis curves, are comprehensively presented in Figs. 2, 3, 4, 5, 6, 7, 8, and 9. Samples (2.5 N, 2 V and 4.5 N, 4 V) subjected to five cycles of heating–cooling were taken and scanning electron microscopy (SEM) was conducted on samples. The SEM images revealed elongated grains, with the black areas representing titanium and the gray areas representing nickel as shown in Fig. 10. Despite the increase in strength and hardness attributed to the elongated grains, it was observed that the higher nickel content compared to titanium rendered the alloy more brittle and prone to fracture during actuation thus decreasing the life cycle.

Conclusion

This paper presented a conducting experiment on a shape memory alloy zigzag sheet with consistent mechanical properties involved the application of various voltage waveforms. Throughout each experiment, data on sheet displacement and temperature was meticulously recorded at intervals of 200 ms, spanning the entire operational lifespan of the sheet under three different weights, 2.5 N, 3.5 N, and 4.5 N, along with three distinct voltage levels—2.0 V, 3.0 V, and 4.0 V. It is found that 2.5 N at voltage level 2 V is optimum condition to obtain maximum life cycle for shape memory alloy zigzag sheet with the displacement of 15.10 mm as in this case there is no

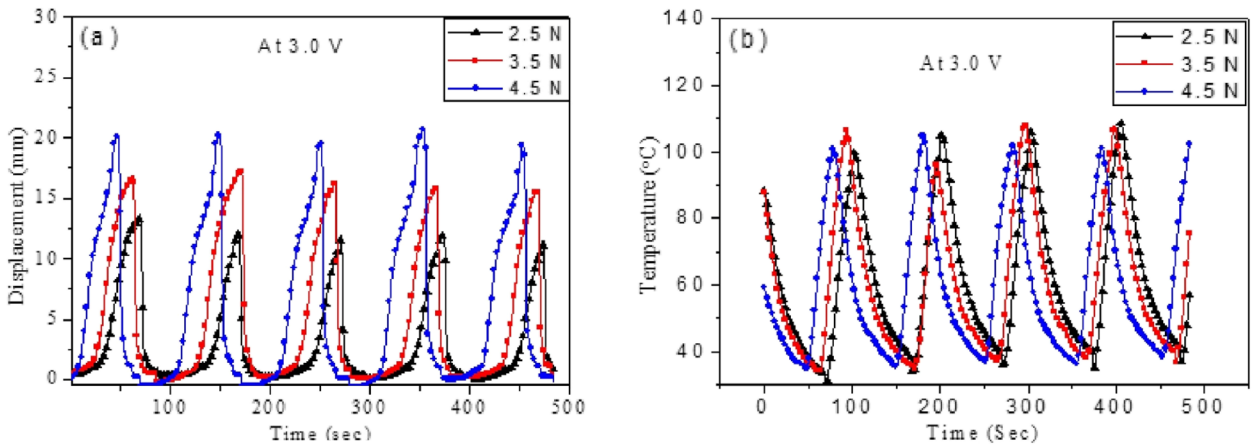

Fig. 5 Displacement vs. time at 3.0 V for different weight **a** for 2.5 N, 3.5 N, and 4.5 N, **b** temperature vs. time plot for 2.5 N, 3.5 N, and 4.5 N

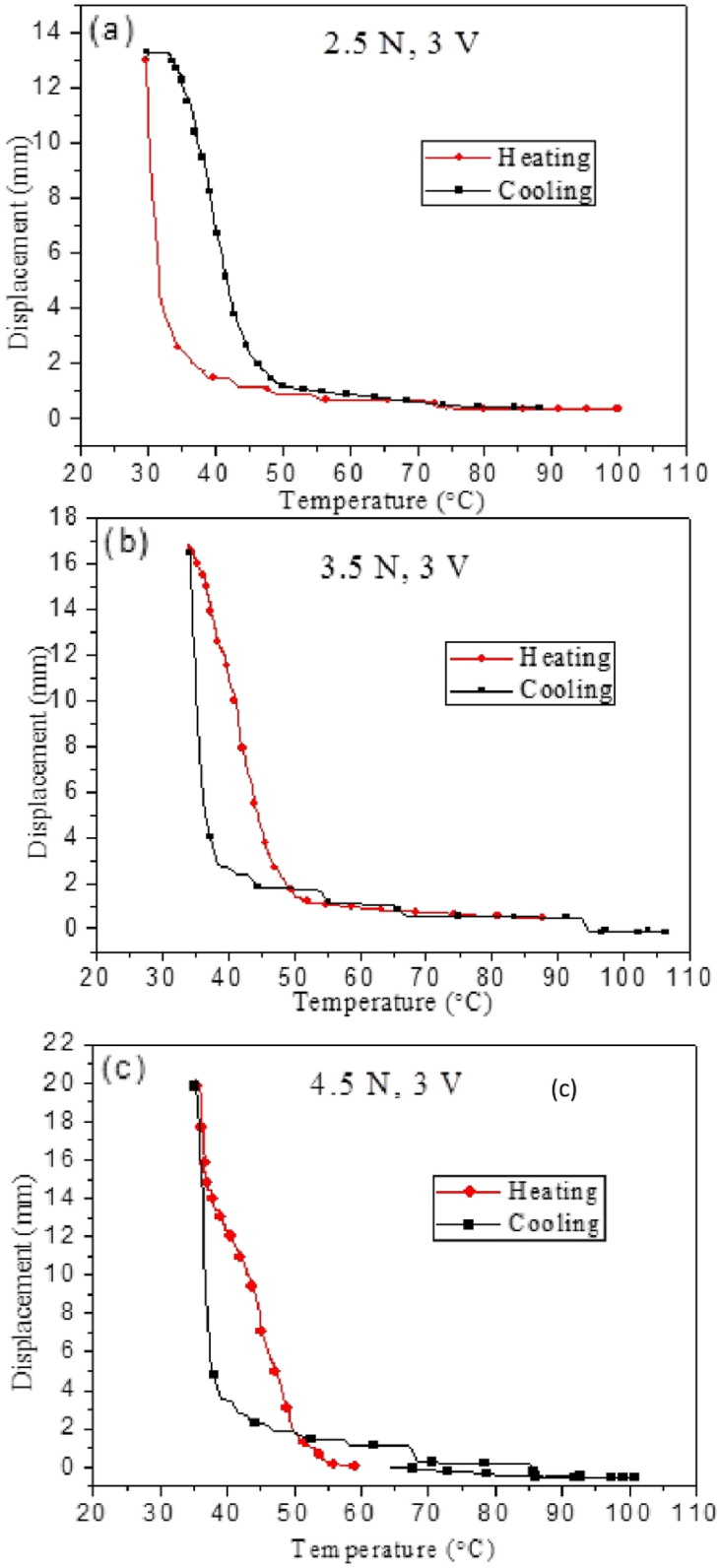

Fig. 6 Hysteresis curve for actuation of SMA at 3.0 V **a** 2.5 N, **b** 3.5 N, **c** 4.5 N

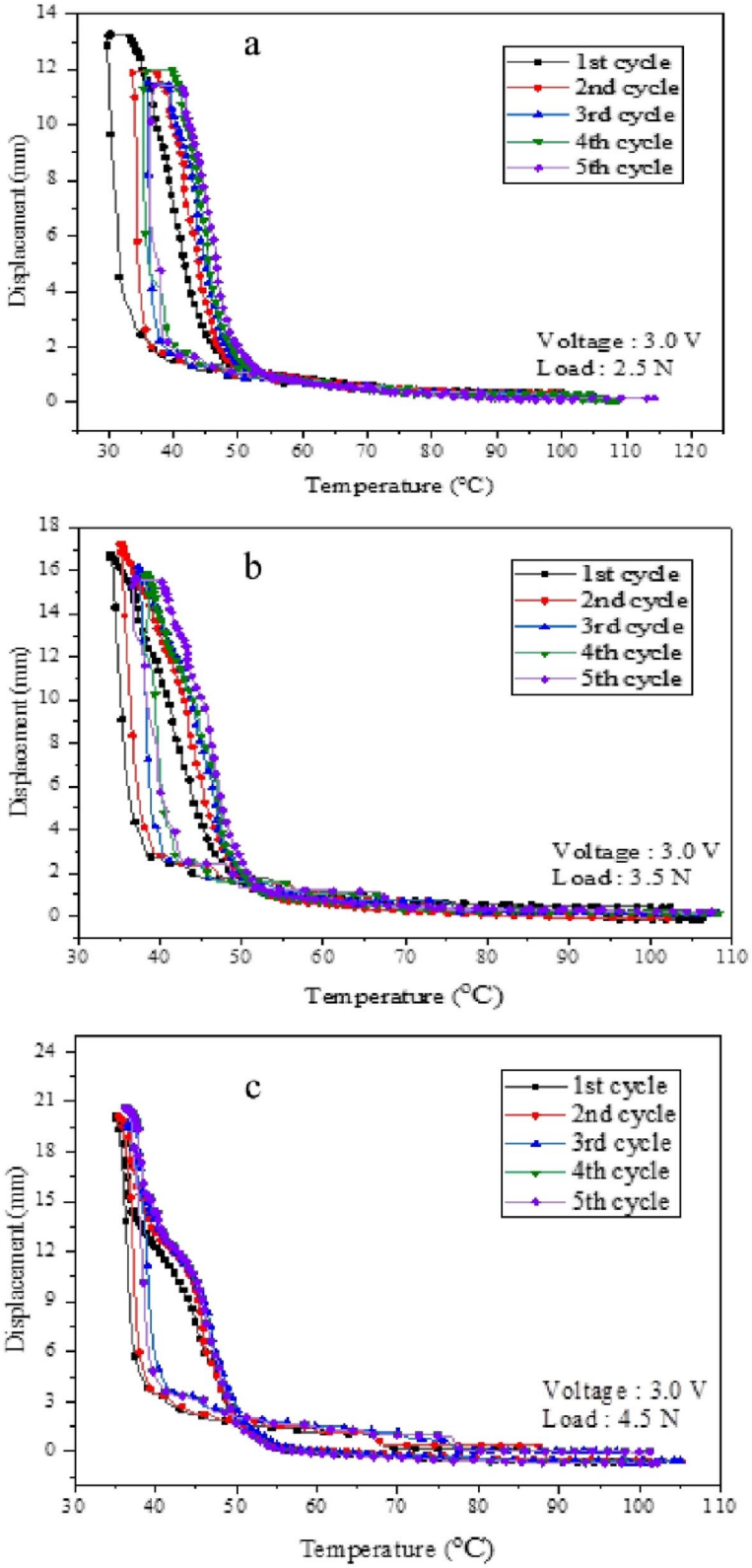

Fig. 7 Hysteresis curves for five cycles are depicted at a voltage of 3.0 V under varying loads: **a** 2.5 N, **b** 3.5 N, and **c** 4.5 N

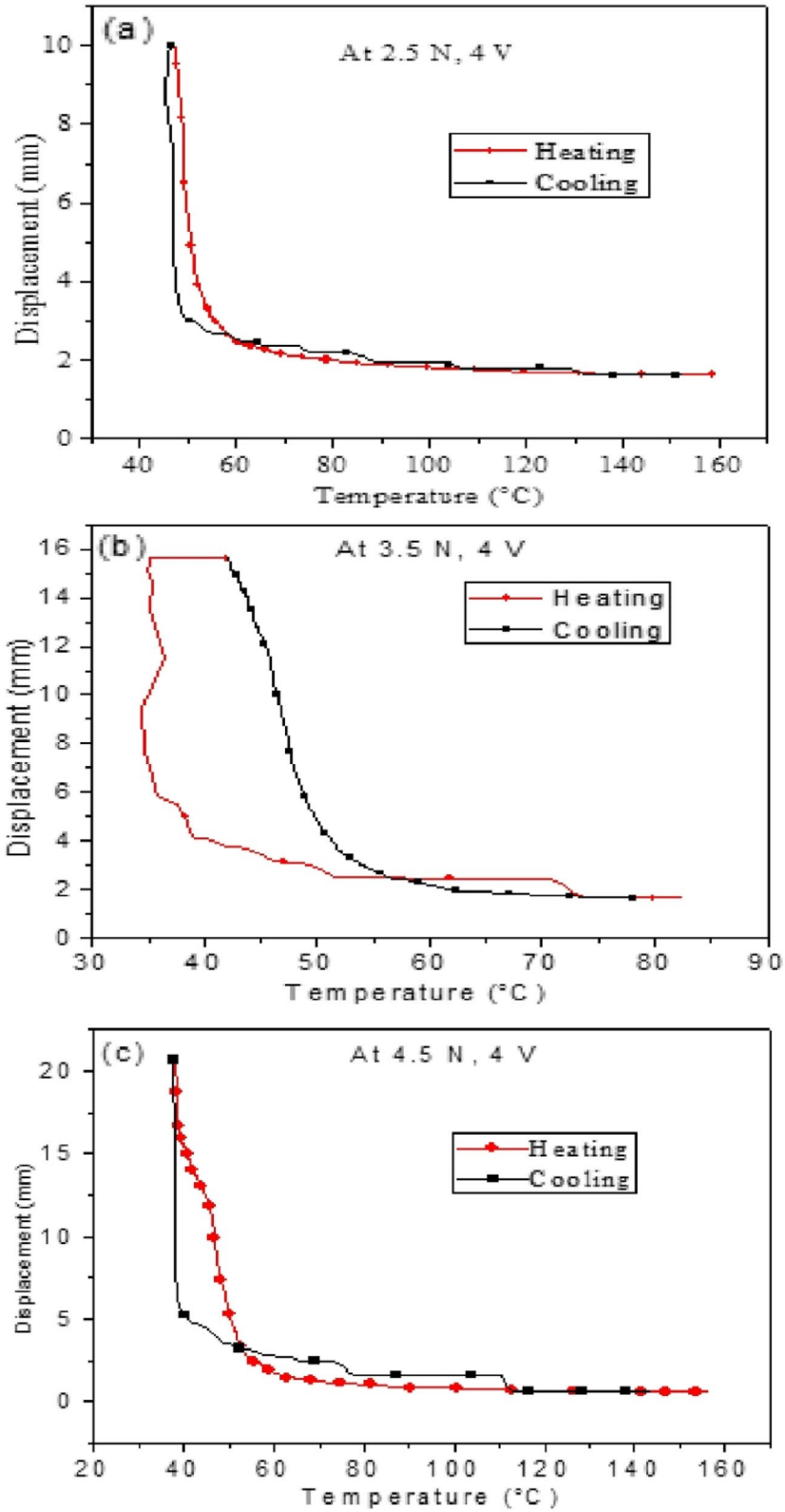

Fig. 8 Hysteresis curve for actuation of SMA at 4.0 V **a** 2.5 N, **b** 3.5 N, **c** 4.5 N

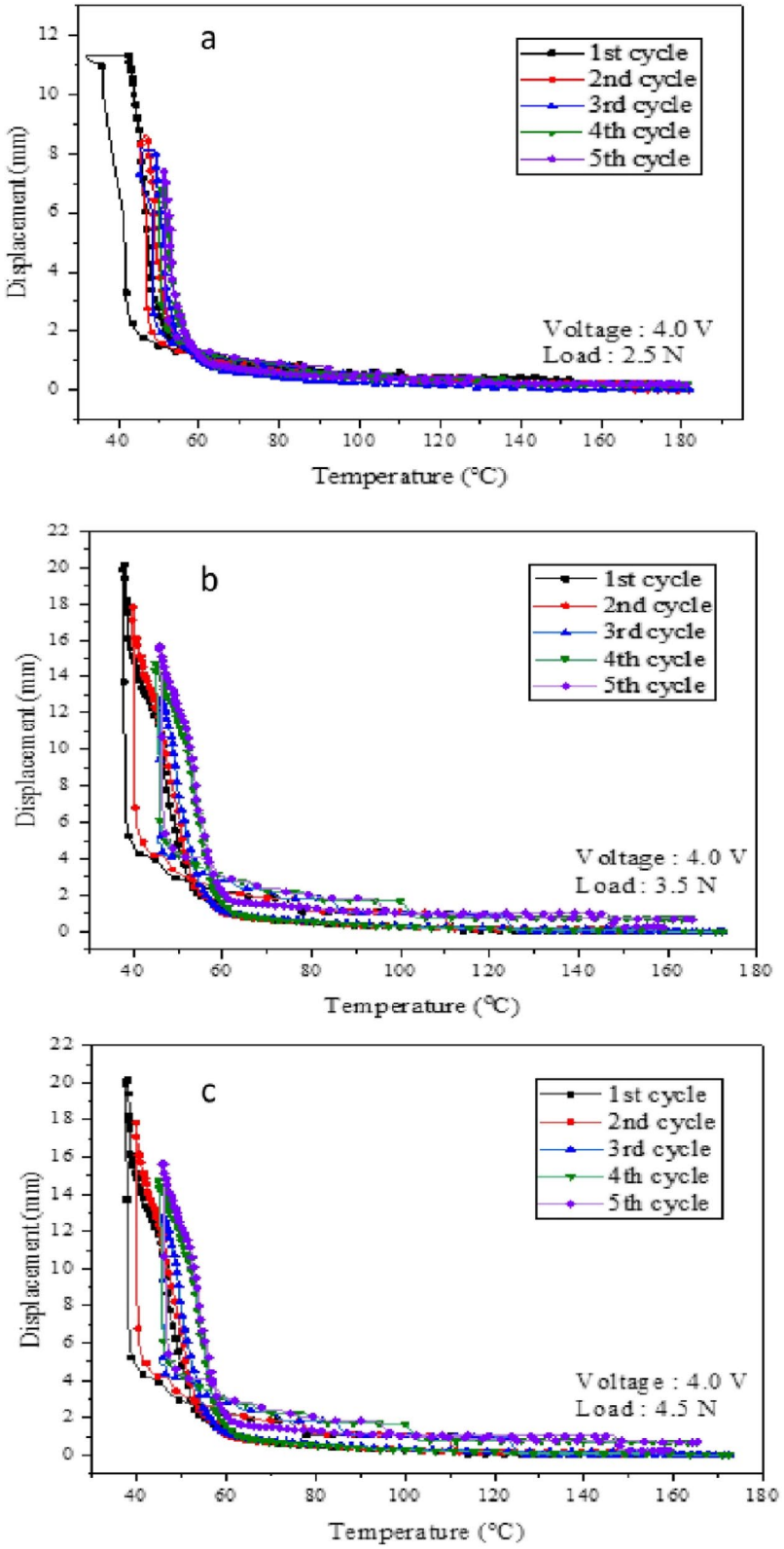

Fig. 9 Hysteresis curves for five cycles are depicted at a voltage of 3.0 V under varying loads: **a** 2.5 N, **b** 3.5 N, and **c** 4.5 N

Table 2 Heating (H) and cooling (C) at different voltages and weights

Parameters	Voltages					
	2 V		3 V		4 V	
Weights						
2.5 N	H-30 s	C-70 s	H-28 s	C-69 s	H-20 s	C-63 s
3.5 N	H-32 s	C-72 s	H-24 s	C-65 s	H-18 s	C-80 s
4.5 N	H-34 s	C-74 s	H-30 s	C-58 s	H-14 s	C-82 s
Displacement	At 2.5 N	15.10 mm	At 3.5 N	18.32 mm	At 4.5 N	21.25 mm

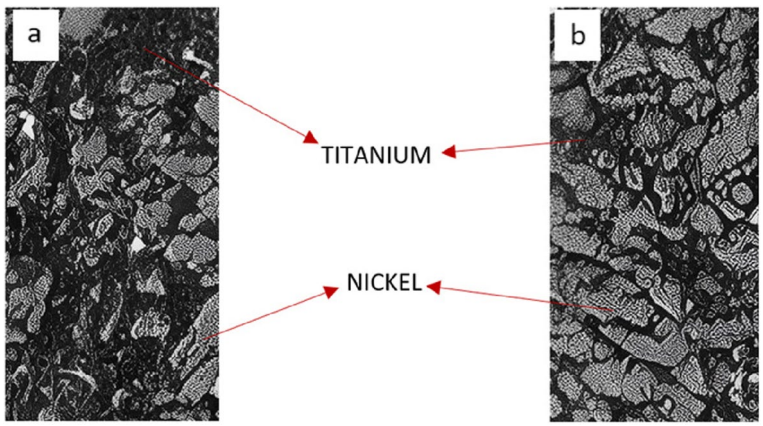

Fig. 10 SEM image of sample (**a** 2.5 N, 2 V and **b** 4.5 N, 4 V) subjected to five cycles of heating and cooling

phase change or temperature change at the time of intersection. As weight and voltage level is increased, life cycle decreases and actuation increases. Result and discussion in this work can be used for future references to design mechanical device using shape memory alloy zigzag sheet. If any device requires higher actuation where life cycle is not the priority, it can be achieved with 4.5 N at voltage level 4 V.

Acknowledgements
I would like to express my heartfelt gratitude to the National Institute of Technology Patna for providing me with excellent research facilities and resources. The support and guidance from the faculty and staff specially to my mentor Dr. Amit Kumar, Professor, Department of Mechanical Engineering, NIT Patna, have been invaluable throughout my research journey. Special thanks to my family, Shipra Saloni, my wife, my twins, Vrishank and Vyom for their constant encouragement and support which significantly contributed to the successful completion of this work.

Authors' contributions
Mr. Suraj performed the experimental work and data analysis and wrote the main manuscript text. Dr. Arun Kumar contributed to data analysis and manuscript revision.

Funding
The authors declare that no funds, grants, or other support were received during the preparation of this experiment and manuscript.

Availability of data and materials
This declaration is "not applicable."

Declarations

Competing interests
The authors declare that they have no competing interests.

Received: 17 June 2024 Accepted: 5 August 2024
Published online: 11 August 2024

References

Bale A. S., Ghorpade N., Hamsalekha R., Pushpanjali J., Deepan W. and Herial J. (2023), "Improved shape memory alloy-based MEMS perforated switch for RF applications," IEEE 12th international conference on communication systems and network technologies (CSNT), Bhopal, India, 2023, pp. 41-45https://doi.org/10.1109/CSNT57126.2023.10134651

Basit A, L'Hostis G, Durand B (2013) High actuation properties of shape memory polymer composite actuator. Smart Mat Struct 22:025023

Cao D, Liu C, Yang Z, Zhang S (2023) A power generation device based on shape memory alloy and piezoelectric ceramic. Mater Chem Phys 301:127598. https://doi.org/10.1016/j.matchemphys.2023.127598

Chang LC, Read TA (1951) Plastic deformation and diffusionless phase changes in metals — the gold-cadmium beta phase. Jom 3(1):47–52. https://doi.org/10.1007/bf03398954

Chaudhary, K., Haribhakta, V. K., & Jadhav, P. V. (2024). A review of shape memory alloys in MEMS devices and biomedical applications. Materials Today: Proceedings. https://doi.org/10.1016/j.matpr.2024.04.105

Chen WM, Liu TS (2013) Modeling and experiment of three-degree-of-freedom actuators using piezoelectric buzzers. Smart Mater Struct 22(10):105006. https://doi.org/10.1088/0964-1726/22/10/105006

Chouhan P, Nath T, Lad BK, Palani IA (2016) Investigation on actuation and thermo-mechanical behaviour of shape memory alloy spring using hot

water. IOP Conf Ser: Mat Sci Engine 149:012147. https://doi.org/10.1088/1757-899x/149/1/012147
Dzogbewu TC, Johan D (2024) Additive manufacturing of NiTi shape memory alloy and its industrial applications. Heliyon 10(1):e23369–e23369. https://doi.org/10.1016/j.heliyon.2023.e23369
Gangwar K, Gupta D, Anand PI (2023) Parametric investigation on laser annealing of polyimide on improving the characteristics of NiTi SMA-based bimorph towards the development of microactuators. Sens Actuators, A 360:114536–114536. https://doi.org/10.1016/j.sna.2023.114536
Grunwald A, Olabi A (2008) Design of a magneto strictive (MS) actuator. Sens Actuators, A 144(1):161–175. https://doi.org/10.1016/j.sna.2007.12.034
Hong C (2013) Application of a magnetostrictive actuator. Mater Des 1980–2015(46):617–621. https://doi.org/10.1016/j.matdes.2012.11.013
Jain, P. K., Sharma, N., Vyas, R., & Jain, S. (2022). Characterization techniques for shape-memory alloys. Springer EBooks, 29–43. https://doi.org/10.1007/978-3-030-94114-7_2
Jayaram K, Jafferis NT, Doshi N, Goldberg B, Wood RJ (2018) Concomitant sensing and actuation for piezoelectric microrobots. Smart Mater Struct 27(6):065028. https://doi.org/10.1088/1361-665x/aabdf1
Kim M, Heo J, Rodrigue H, Lee H, Pané S, Han M, Ahn S (2023) Shape memory alloy (SMA) actuators: the role of material, form, and scaling effects. Adv Mater 2023(35):2208517. https://doi.org/10.1002/adma.202208517
Lagoudas DC (2008) Shape memory alloys. Springer Science & Business Media, New York
Mehta A, Singh G, Vasudev H (2024) Processing of shape memory alloys research, applications and opportunities: a review. Phys Scr 99(6):062006–062006. https://doi.org/10.1088/1402-4896/ad48cb
Mobarak MH, Aminul Islam Md, Hossain N, Mahmud A, Thohid Rayhan Md, Nishi NJ, Chowdhury MA (2023) Recent advances of additive manufacturing in implant fabrication – a review. Appl Surface Sci Adv 18:100462–100462. https://doi.org/10.1016/j.apsadv.2023.100462
Mohd Jani J, Leary M, Subic A (2016) Designing shape memory alloy linear actuators: a review. J Intell Mater Syst Struct 28(13):1699–1718. https://doi.org/10.1177/1045389x16679296
Moiseev VN (2005) Titanium in Russia. Met Sci Heat Treat 47(7–8):371–376. https://doi.org/10.1007/s11041-005-0080-9
Namazu T, Tashiro Y, Inoue S (2006) Ti–Ni shape memory alloy film-actuated microstructures for a MEMS probe card. J Micromech Microeng 17:154–162
Nath T, Kumar S (2021) "Nitinol shape memory alloy spring." Ind J Engine Mat Sci IJEMS (CSIR) 28(5):446–453
Nithyanandh G, Yogeshwaran SK, Santosh S (2023) Preparation, characterization and dynamic mechanical analysis of CuZnAl shape memory alloys. Mat Today Proc 72:2476–2479. https://doi.org/10.1016/j.matpr.2022.09.514
Patil D, Song G (2017) A review of shape memory material's applications in the offshore oil and gas industry. Smart Mater Struct 26(9):093002. https://doi.org/10.1088/1361-665x/aa7706
Pelrine R, Kornbluh R, Joseph J (1998) Electrostriction of polymer dielectrics with compliant electrodes as a means of actuation. Sens Actuators A: Phys 66:77. https://doi.org/10.1016/s0924-4247(97)01657-9
Pimpin, A., Suzuki, Y., & Kasagi, N. 2004. Micro electrostrictive actuator with metal compliant electrodes for flow control applications. 17th IEEE international conference on micro electro mechanical systems. Maastricht MEMS 2004 technical digest. https://doi.org/10.1109/mems.2004.1290626
Shape memory alloys - new advances [working title]. (2023). IntechOpen EBooks. https://doi.org/10.5772/intechopen.111044
Sun J, Guan Q, Liu Y, Leng J (2016) Morphing aircraft based on smart materials and structures: a state-of-the-art review. J Intell Mater Syst Struct 27(17):2289–2312. https://doi.org/10.1177/1045389x16629569
Sun L, Huang W, Ding Z, Zhao Y, Wang CC, Purnawali H, Tang C (2012) Stimulus-responsive shape memory materials: a review. Mat Design 33:577. https://doi.org/10.1016/j.matdes.2011.04.065
Takashima K, Sugitani K, Morimoto N (2014) Pneumatic artificial rubber muscle using shape-memory polymer sheet with embedded electrical heating wire. Smart Mater Struct 23(12):125005. https://doi.org/10.1088/0964-1726/23/12/125005
Teh, Y. H. 2008. Fast, accurate force and position control of shape memory alloy actuators. https://doi.org/10.25911/5d626e133157c
Yuan H, Fauroux J, Chapelle F, Balandraud X (2017) A review of rotary actuators based on shape memory alloys. J Intell Mater Syst Struct 28(14):1863–1885. https://doi.org/10.1177/1045389x16682848

Publisher's Note